Current Problems in Diagnostic Radiology 48 (2019) 379–386

Current Problems in Diagnostic Radiology

journal homepage: www.cpdrjournal.com

Molecular Imaging in Diagnosis of Tumor-induced Osteomalacia

Ming Yang, MD[a,*], Krupa B. Doshi, MD[b], Michael C. Roarke, MD[a], Ba D. Nguyen, MD[a]

[a] Department of Radiology, Mayo Clinic, AZ
[b] Division of Endocrinology, Department of Internal Medicine, Mayo Clinic, AZ

Tumor induced osteomalacia (TIO) is a rare paraneoplastic syndrome caused by overproduction of fibroblast growth factor 23 (FGF23) secreted by benign mesenchymal neoplasm. Due to its nonspecific clinical presentation or lack of awareness, the diagnosis of TIO is often significantly delayed resulting in patients' prolonged physical suffering or psychological distress. Successful detection or complete surgical resection of the causative tumor typically leads to rapid resolution of symptoms or reversal of biochemical imbalance. Nuclear medicine and molecular imaging have been playing a promising role as the first-line imaging modalities in the diagnosis and localization of occult FGF23 secreting mesenchymal tumor, especially with the emerging whole-body, head-to-toe Ga68-DOTATATE PET/CT technique. Combined focused diagnostic CT and/or MRI are imperative for accurate delineation of tumor and surgical guidance.

Introduction

Tumor-induced osteomalacia (TIO), also known as oncogenic osteomalacia, is an uncommon paraneoplastic syndrome with abnormal metabolism of phosphate and vitamin D.[1,2] Main characteristics of TIO are hypophosphatemia, renal phosphate wasting, and osteomalacia.[3] In 2001, overproduction of fibroblast growth factor 23 (FGF23) by benign mesenchymal tumors was identified as the causative mechanism.[4] Patients with TIO present with slow but steady progression of generalized skeletal pain, muscular weakness, height loss, recurrent fractures, and sequential psychological distress. Due to its nonspecific clinical presentation, rare occurrence, and general lack of clinical awareness of this disease, TIO may often be mistaken for other musculoskeletal or neurologic disorders, and its diagnosis is often significantly delayed thereby.[5] Successful detection and complete surgical removal of the causative tumor typically leads to rapid resolution of symptoms and reversal of biochemical imbalance within days to weeks after surgery.[6-8] Hence, prompt and accurate identification of the FGF23 secreting tumor is an important step in the clinical diagnosis and management of TIO.

In this pictorial review, through illustration of multimodality imaging features of FGF23 secreting phosphaturic mesenchymal tumors, our aim is to (1) raise the awareness of TIO in clinical practice, (2) summarize the radiologic manifestations of combined functional and morphologic imaging modalities, and (3) recommend the utility of whole body positron emission tomography (PET)/computed tomography (CT), especially that of the evolving somatostatin receptor analogue-based Ga68-DOTATATE PET tracer, as the first line imaging modality in the localization and diagnosis of this rare clinical disorder.

Epidemiology

TIO was first described by Robert McCance in 1947.[9] Since then, there have been over 300 published case reports and small cohort studies regarding this condition, with the majority being published after year 2001, when FGF23 was identified as the causative phosphaturic agent.[10,11] After reviewing 269 TIO cases published in medical literature and 39 cases diagnosed at their institution, Jiang et al. found an equal gender and age distribution of TIO with 47% in women and 53% in men, mean age 45 ± 16 years (range 2-86 years). Among the reported cases, 40% of causative mesenchymal tumors were located in bone and 55% in soft tissue. The remaining cases either had unidentified tumors or tumors located at multiple sites.[11] For skeletal tumor, common sites included thigh (22.7%), craniofacial region (20.7%), hand and foot (8.8%), pelvis (8.2%), tibia and/or fibula (6.5%), and arms (6.5%).[12] Since the majority of reported tumors were of small size and slow growing nature, and located at atypical sites, the detection and localization of these tumors was a challenging task.[13]

Phosphate Homeostasis

Phosphate plays a vital role in skeletal development, energy metabolism, and bone mineralization, as well as in numerous intracellular molecular metabolic pathways.[14,15] Phosphate is predominantly stored within the skeleton. Serum phosphate level is maintained through renal tubular and intestinal reabsorption, and exchanges with intracellular and bone storage pools. It has been well recognized that serum phosphate concentrations are regulated mainly by parathyroid hormone (PTH), and to a lesser degree, by 1, 25-dihydroxy vitamin D.

Disclosure: All listed authors have been aware of the instructions or ethical responsibility related to publication on your journal, or agreed to comply with related policy. There is no conflict of interest either.
Funding: No funding support for this manuscript.
*Reprint requests: Ming Yang, MD, Department of Radiology, Mayo Clinic in Arizona, 13400 E Shea Blvd, Scottsdale, 85259 AZ.
E-mail address: yang.ming@mayo.edu (M. Yang).

https://doi.org/10.1067/j.cpradiol.2018.06.005
0363-0188/

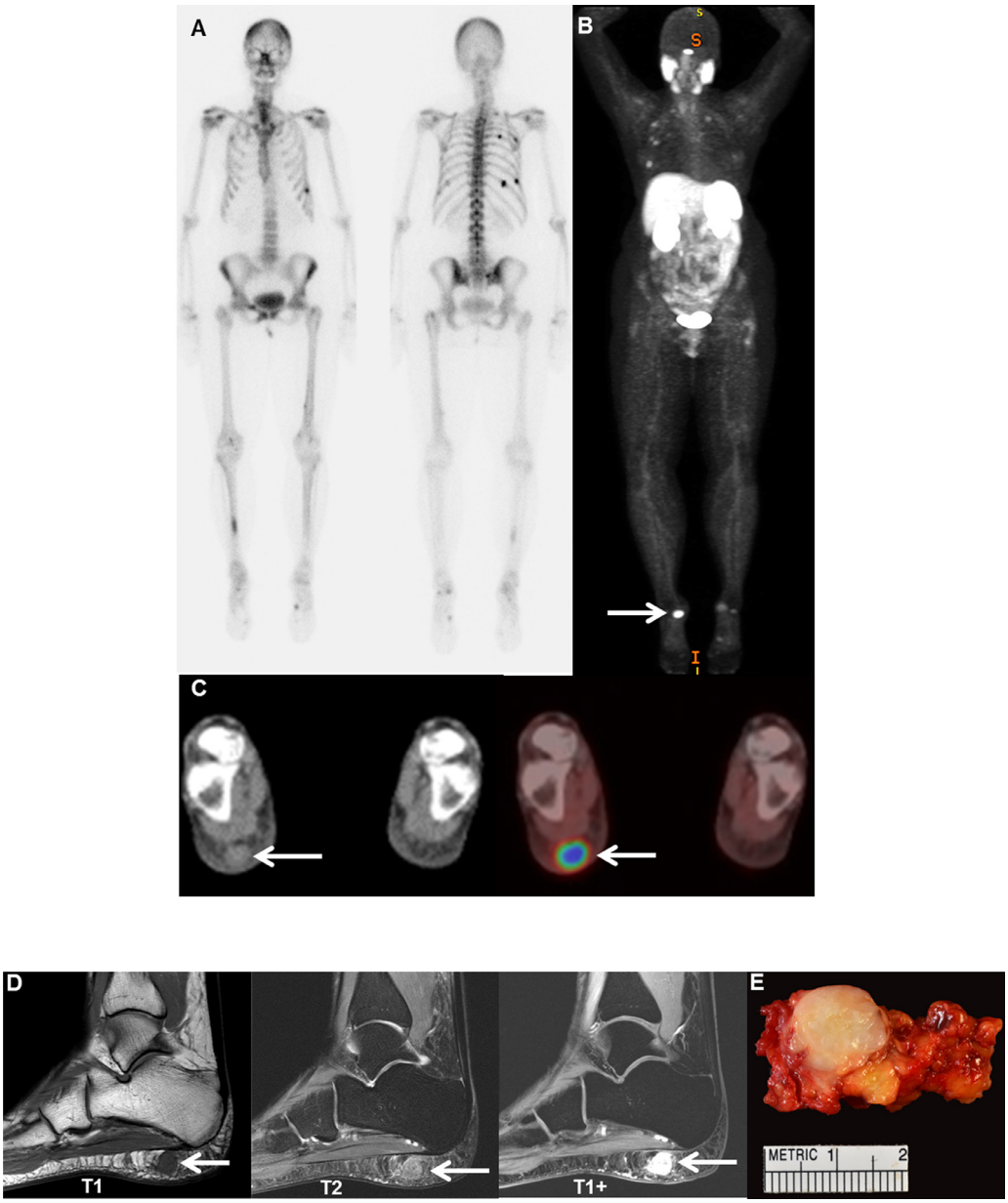

FIG 1. Right heel tumor. A 60-year-old female patient presented with multiple fractures in the past several years. Her FGF23 was 266 RU/ml (normal range <180 RU/ml). Tc-99m whole-body bone scintigraphy showed multiple fractures (A) Ga68-DOTATATE PET/CT was notable for a 1.6 × 1.2 cm tracer avid soft tissue density nodule in the right foot plantar subcutaneous region (B, PET MIP; C axial images, arrows), and multiple insufficient fractures in bilateral rib cages. On foot MRI, the right heel subcutaneous nodule exhibited isointense to muscle T1 signal, highT2 signal and heterogeneous enhancement (D, arrows). The patient underwent total tumor resection, with pathologically proven benign phosphaturic mesenchymal tumor, positive for FGF23 mRNA expression (E). The serum FGF23 dropped to 50 RU/ml after surgery. (Color version of figure is available online.)

In 1989, "phosphatonin" FGF23 was discovered by Meyer et al.[16] as the responsible circulating hormonal factor for renal phosphate wasting in mice. Under physiologic conditions, FGF23 is secreted by bone and degraded by proteolytic enzymes.[17] In TIO, excessive secretion of FGF23 by tumors causes the reduction of NaPi-2a transcription, and consequently leads to abnormally increased renal phosphate excretion and severe hypophosphatemia.[18,19] Therefore, hyperphosphaturia and low serum phosphorus levels with normal calcium, 25-hydroxy vitamin D and creatinine, as well as elevated serum FGF23, are biochemical hallmarks of this clinical entity.

Histopathology Manifestation

FDG 23 secreting tumors are typically benign mesenchymal neoplasms. Weidner and Folpe et al. first classified this group of tumors as phosphaturic mesenchymal tumors with a mixed connective tissue variant featured as a spindled-to-satellite tumor cell with small nuclei and indistinctive nucleoli under microscope. The most frequently diagnosed phosphaturic mesenchymal tumor was hemangiopericytoma, which consisted of 70%-80% TIO cases, followed by hemangioma, ossifying fibroma, granuloma, and giant cell tumor.[1,2,20-22] In addition, Folpe et al. found that 70% of mesenchymal tumors presented with positive FGF23 immunohistochemistry staining in actively proliferative tumor cells. Variable degrees of somatostatin receptor (SSTR) subtype 2 expressions were also identified in many tumors.[2,8,23,24]

Differential Diagnosis

Once the diagnosis of TIO is confirmed, a thorough history and physical examination can aid in the differential diagnosis and distinguish it from other genetic causes. The differential diagnosis of TIO

includes X-linked hypophosphatemic rickets and autosomal-dominant hypophosphatemic rickets. In X-linked hypophosphatemic rickets, the mutated *PHEX* (a phosphate-regulating gene with homologies to endo peptides located on the X chromosome) leads to ineffective FGF23 proteolytic breakdown, and in autosomal-dominant hypophosphatemic rickets, the mutated FGF23 prevents normal breakdown by *PHEX*.[25-27]

Nuclear Medicine and Molecular Imaging in Detection of Tumor

Lesions responsible for TIO can occur anywhere in the body and mainly involve bone, soft tissue, and skin. Complete removal of the tumor usually leads to rapid resolution of symptoms and reversal of biochemical hallmarks. Consequently, radiographic imaging detection and localization of these tumors play a crucial role in guiding surgery.[28] A stepwise approach has been advocated in combination with functional and morphologic imaging modalities to locate the FGF23 secreting tumor.[10] Using this approach, whole-body scintigraphy or PET/CT imaging was utilized to discover the suspicious tumor through a radiotracer's distinguished metabolic pathway, followed by high resolution radiologic imaging modalities, including X-ray radiography, cross-sectional CT, and magnetic resonance imaging (MRI) to provide detailed anatomical tumor localization for surgery. Multiple radiopharmaceuticals have been investigated in the detection of tumors in TIO, including technetium (Tc)-99m methyldiphosphonate (MDP),[29,30] Tc-99m sestamibi,[31] thallium

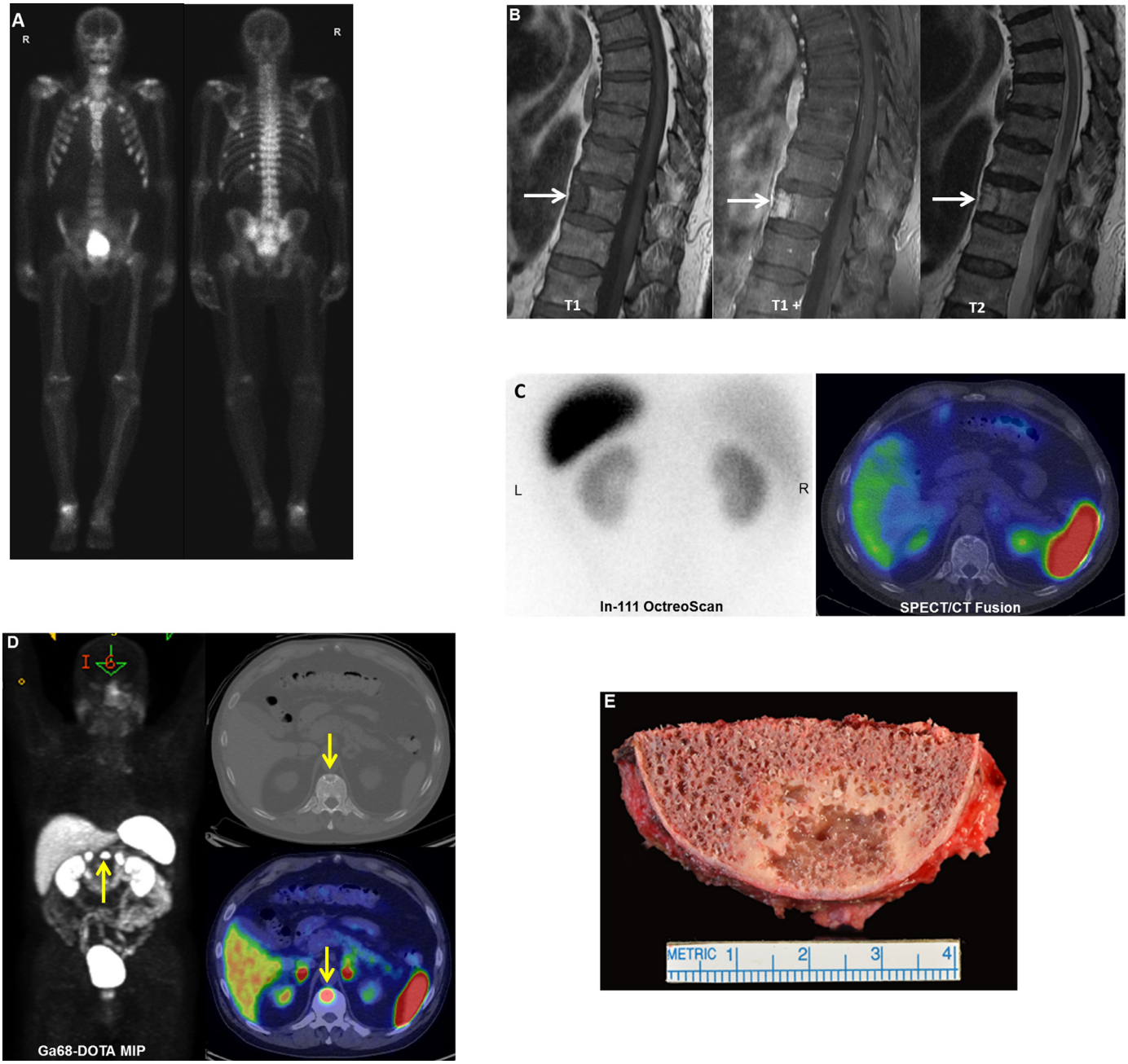

FIG 2. Thoracic spine vertebral tumor. A 70-year-old male patient with history of prostate cancer complained of persistent muscle aches, joint aches, and weakness over the past couple of years. Laboratory test revealed hypophosphatemia and elevated FGF23 at 930 RU/ml. Whole-body bone scintigraphy revealed multiple rib and extremity fractures not related to prostate cancer (A). Spine MRI revealed a focal lesion at the anterior portion of the T11 vertebral body, with MR signal pattern suggesting an atypical meningioma (B, arrows). This lesion did not take tracer on In-111 pentetreotide scintigraphy (Octreoscan) (C). However, it demonstrated intense tracer uptake on Ga68-DOTATATE PET/CT (D, arrows). The patient underwent a partial corpectomy of T11 (E) with a pathologically proven benign phosphaturic mesenchymal tumor. His FGF23 level dropped to 78 RU/ml immediately after surgery. (Color version of figure is available online.)

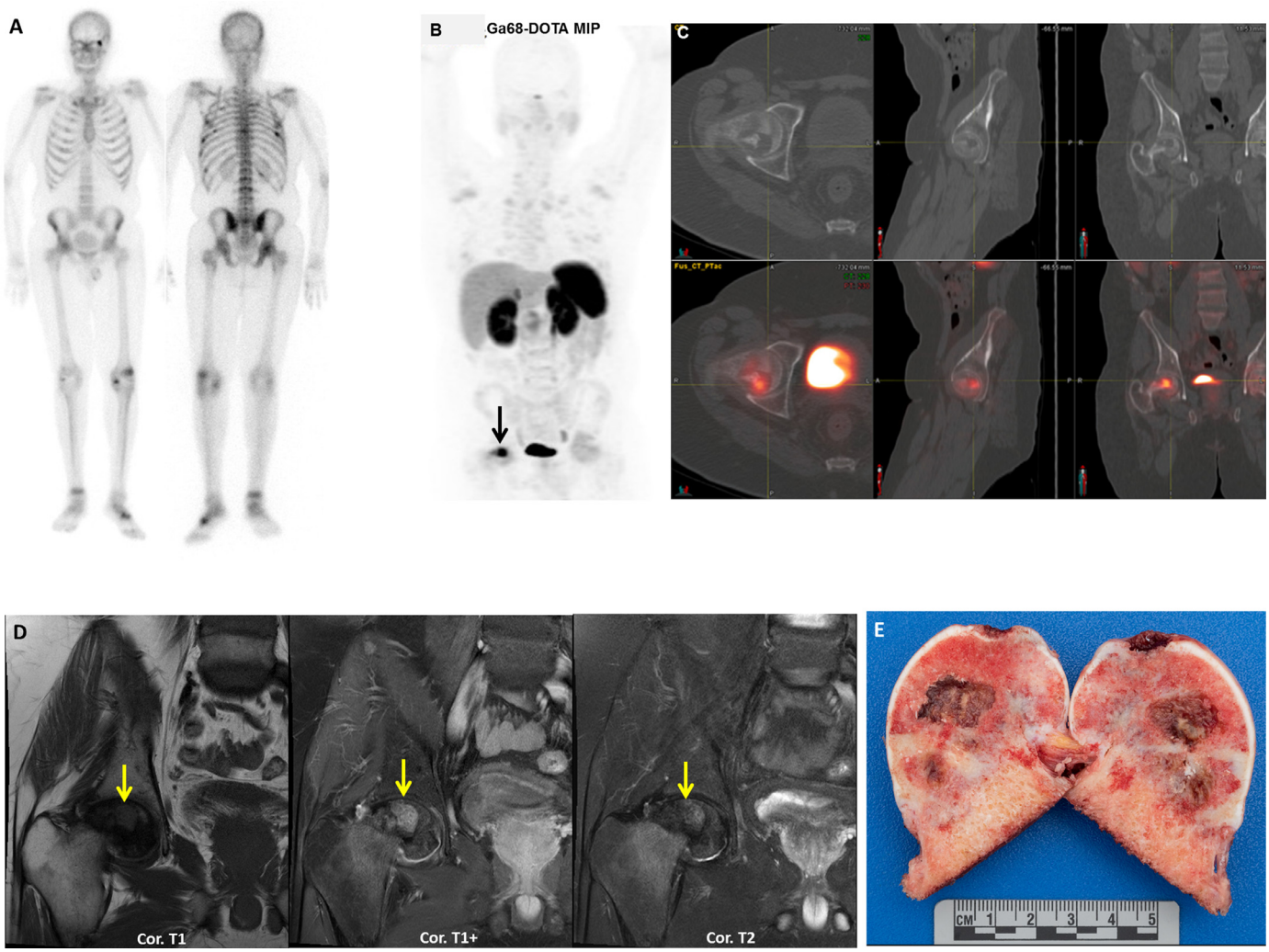

FIG 3. Right femoral neck tumor. A 37-year-old former healthy male runner presented with debilitating bone pain and progressive generalized weakness needing assistance of a rolling walker for ambulation over the past several years. Laboratory tests showed severe hypophosphatemia and very high FGF23 of 910 RU/mL. Whole-body bone scintigraphy showed multiple fractures involving the rib and focal intense tracer uptake at the right femoral neck (A) Ga68-DOTATATE PET/CT showed a dominant right femoral head lucent lesion with central irregular shaped calcification demonstrating increased tracer uptake (B, arrow; C, cross-hair). On MRI, this lesion demonstrated T1 hypointensity, T2 hyperintensity, and heterogeneous enhancement (D, arrows). The patient received right total hip replacement (E) with a pathologically proven benign phosphaturic mesenchymal tumor. His FGF23 dropped to 161 RU/ml at day 1 postsurgery. (Color version of figure is available online.)

(TI)-201, and indium(In)-111 pentetreotide scintigraphy (Octreo-Scan) with and without single-photon emission computed tomography (SPECT)/CT,[32] F18-fluorodeoxyglucose (FDG) PET/CT,[33-35] and evolving Ga68-DOTA–based somatostatin analogue PET/CT.[7,8]

Tc-99m MDP Bone Scintigraphy

Tc-99m MDP bone scintigraphy is a well-established technique utilized in nuclear medicine for detection of osteoblastic processes in the skeleton, especially metastasis secondary to prostate and breast cancer, etc. In adults with TIO, Tc-99m MDP bone scans often reveal diffuse osteomalacia and related insufficient fractures (Figs 1A, 2A, 3A, and 6A).[29,30] However, nonspecific scintigraphy findings may mimic metastatic bone lesions and other metabolic etiologies, including malabsorption, renal failure, vitamin D deficiency, and drug abuse.[30] In both medical literature and our practice, Tc-99m MDP whole body bone scintigraphy alone seldom discerns the causative tumor in TIO, and sometimes it even misdirects clinical efforts.[29,36]

In addition, Tc-99m sestamibi and TI-211 radiotracer have been used in tumor detection in TIO and are found to be helpful in some clinical scenarios (Figs 5A and 6C). Although the exact mechanism is unclear, it is assumed that vigorous FGF23 secretion occurs in tumors of TIO. These tumors are often hypercellular, which thereby leads to increased accumulation of both radiotracers on scintigraphy images. Combined with the advanced SPECT/CT technique, the tumor detection rate improves.[31,32]

F18-FDG PET/CT

F18-FDG, a competitive glucose analogue, has been advocated for localization of the tumor in TIO based on increased glucose metabolism of the tumor cell.[33,34] The whole body 3-dimensional image reconstruction technique with excellent co-registration between PET and CT images provides a superb preoperative mapping of phosphaturic tumors, facilitates the detection of occurrences at unanticipated sites, and guides the surgical management (Figs 4A, 4B and 6B). Jagtap and colleagues scanned 8 TIO patients using F18-FDG PET/CT and detected tumors in 7 of them, with 4 patients confirmed positive for mesenchymal tumor on histopathology, 1 patient false positive, and 2 patients negative. The slow-growing nature of this group of tumors and the variable degree of tracer uptake of FDG might be accountable for the unsatisfactory detection rate.[34]

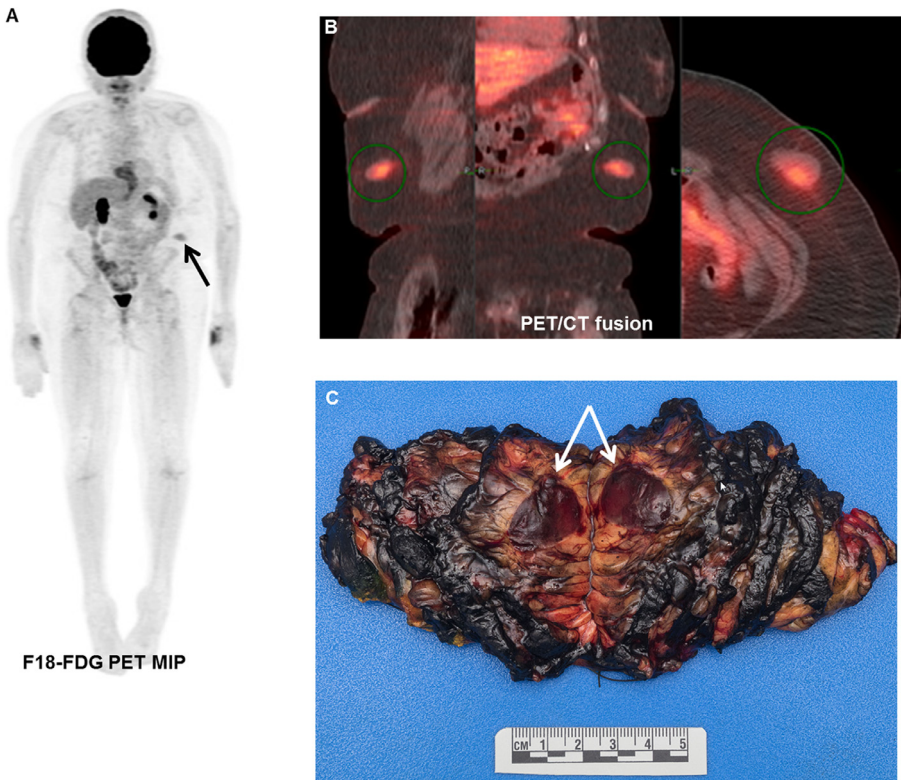

FIG 4. Abdominal wall tumor: A 47-year-old female with over 10-year history of nontraumatic fractures and renal stones was noted to have hypophosphatemia and elevated FGF23 at 1270 RU/ml even after parathyroidectomy. The patient noticed a left abdominal wall mass. Whole-body F18-FDG PET/CT demonstrated a subcutaneous soft tissue density lesion with mildly increased FDG uptake, maximal SUV 3.1 (A, arrow; B, circles). The patient underwent left anterior abdominal wall wide-margin local excision (C) of a pathologically proven benign phosphaturic mesenchymal tumor with positive FGF23 mRNA expression. The serum FGF23 dropped to 132 RU/ml shortly after surgery. (Color version of figure is available online.)

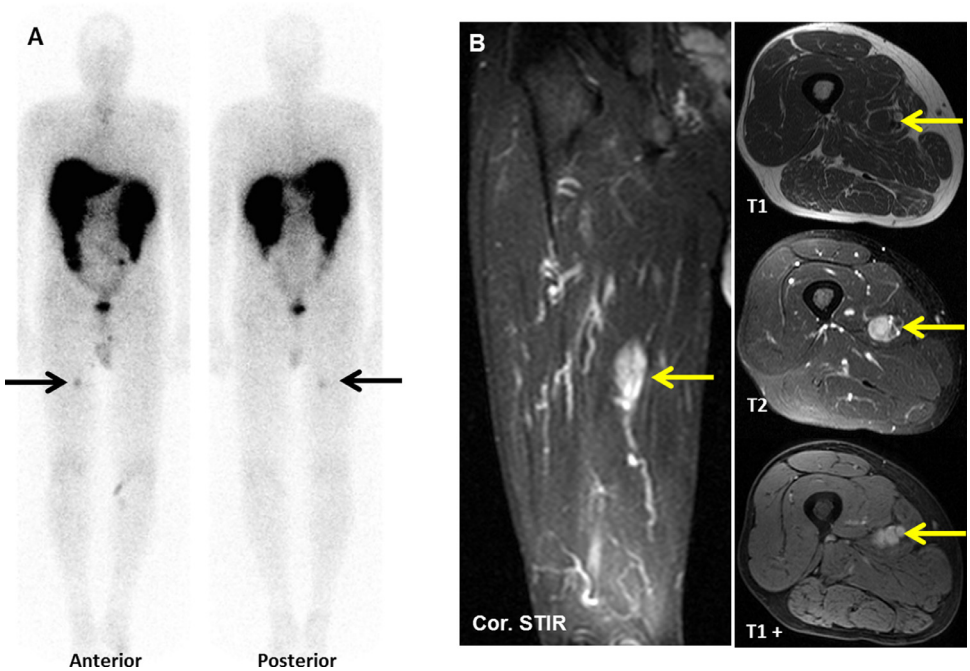

FIG 5. Right thigh intramuscular tumor. A 53-year-old male presented with chronic hypercalcemia and hypophosphatemia. Indium-111 OctreoScan showed a focal abnormal tracer uptake within the proximal right thigh (A, arrows) suspicious for a lesion with somatostatin-receptor expression. Coronal inversion recovery and axial MR images showed a mass within the medial aspect of the proximal right thigh (B, arrows). This lesion was a pathologically proven phosphaturic mesenchymal tumor. The patient's laboratory biomarkers came back to normal after surgery, however, FGF23 level was not drawn prior to surgical resection. (Color version of figure is available online.)

In-111 penterotide scintigraphy and Ga68-DOTATATE PET/CT

SSTRs have been found on the cell membrane of active FGF23 secreting tumors with variable degrees of expression, which allows for visualization of phosphaturic neoplasms using SSTR scintigraphy imaging.[37] The In-111-labeled pentetreotide has a high affinity to SSTR 2, and to a lesser extent, to SSTR 5. Multiple reports have shown clinical success of OctreoScan with combined SPECT/CT in detection

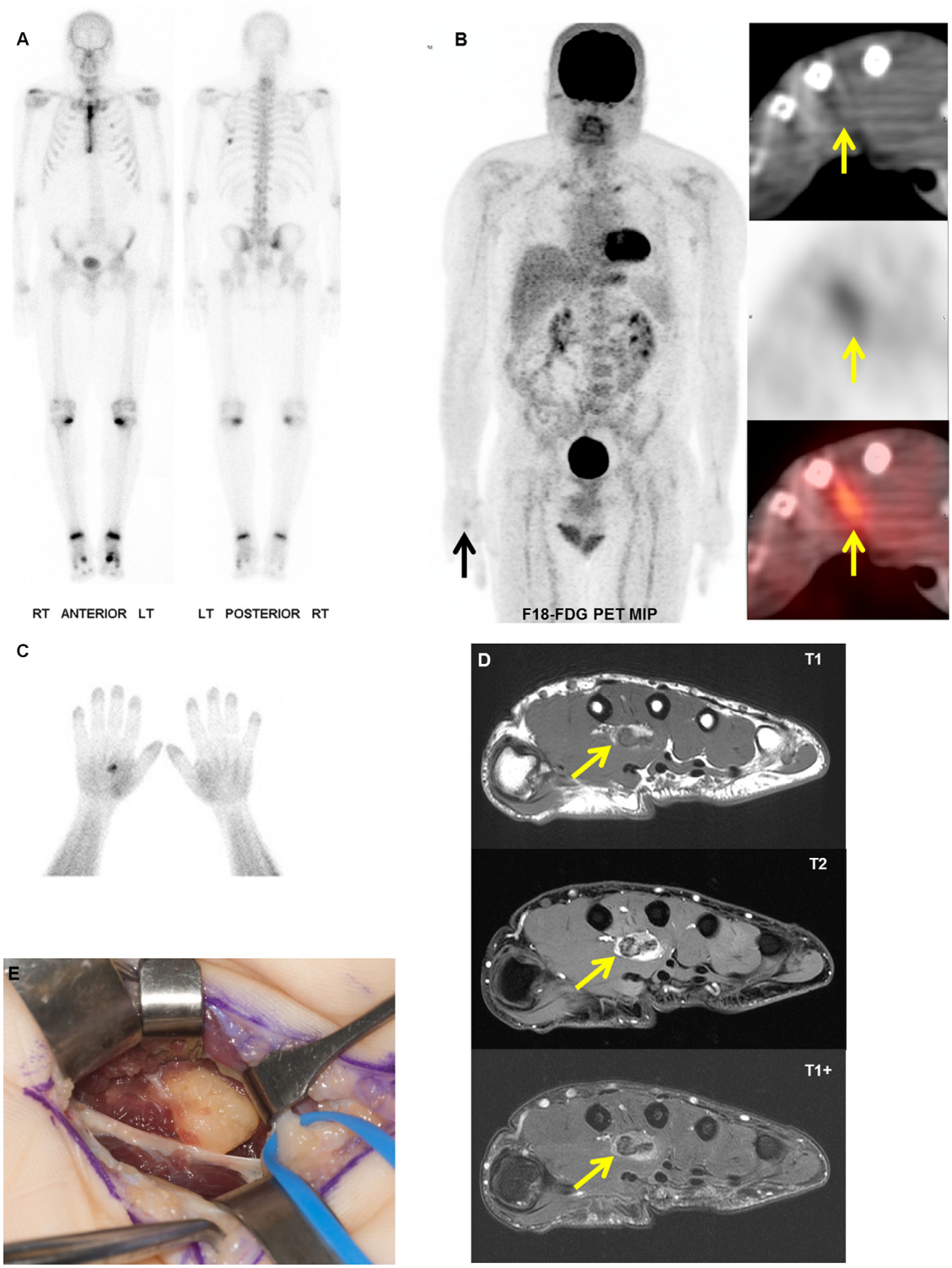

FIG 6. Right palm tumor. A 53-year-old male presented with generalized muscle pain and a left metatarsal fracture. Laboratory workup demonstrated marked hypophosphatemia and elevated FGF23 at 455 RU/ml. Extensive imaging workup ensued. Tc-99m MDP bone scintigraphy revealed fractures at various stages involving the ribs, left first metatarsal area, and bilateral tibias (A) Initial PET/CT interpretation overlooked a faint focus of F-18 FDG uptake of the right palm (B, PET MIP and PET/CT spot views of the right hand, SUVmax 2.4, arrow). Due to the persistent laboratory results suggestive of TIO, a subsequent Tc-99m sestamibi scan was obtained showing the suspicious right hand focal increased uptake (C) On the right-hand MRI, this focus represented a 1.9 cm × 1.8 cm × 1.2 cm heterogeneously signaling and enhancing ovoid soft tissue nodular lesion embedded in the right palm soft tissue (D) The intraoperative photo of the right palm circumscribed tumor (E) showed a pathologically proven phosphaturic mesenchymal tumor. (Color version of figure is available online.)

of FGF23 secreting mesenchymal tumors. False-negative findings may be related to small lesion size, poor spatial resolution of planar scintigraphy, suboptimal expression of SSTR, or adjacent location of bone fracture (Fig 2C).[8,36,38]

Recently, SSTR PET/CT imaging based on Ga68 labeled DOTA-conjugated peptides, DOTATATE, DOTATOC, and DOTANOC, has emerged as a promising imaging modality in localizing mesenchymal tumors causing TIO.[24,39,40] Among these peptides, the Ga68-DOTATATE has

demonstrated superior spatial resolution and improved specificity by solely targeting SSTR 2 expressed on tumor cell surface.[7,8,41] Ga68-DOTATATE PET/CT not only aids in visualizing the culprit tumor, but also allows us to quantitatively evaluate the intensity of the affinity between the DOTATATE analogue and tumor cell surface of the SSTR 2 receptor in terms of standard uptake value (SUV). False positive etiologies (ie, osteomalacia-induced fractures) also present with increased SUV and could occasionally be confusing in the localization of primary tumors (Figs 1B, 2D, 3B and 3C). Cautious visual inspection and evaluation of tumor tracer uptake intensity, as well as correlation with CT findings might aid in distinguishing tumors from confounding etiologies.[36]

Direct comparison of F18-FDG PET/CT and Ga68-DOTATATE PET/CT has been conducted to evaluate their performance in tumor localization in a small cohort of TIO patients.[42] Ga68-DOTATATE PET/CT out performed F18-FDG PET/CT in the detection of mesenchymal tumors in 5 of 6 (83%) patients. The superiority of Ga68-DOTATATE may lie on its increased specificity by targeting SSTR 2 expressed on the tumor cell surface. On the other hand, benign and slow growing mesenchymal tumors usually express variably low-grade FDG uptake and can be difficult to distinguish from other etiologies and physiologic uptake. Therefore, it is not surprising that Ga68- DOTATATE PET/CT detects more lesions than F18-FDG PET/CT.

Treatment

Complete surgical resection of the FGF23 secreting tumor is curative and leads to rapid clinical recovery, reversal of biochemical hallmarks, healing of the skeletal sequelae, and relief of associated psychological stress.[8,43,44] In a minority of cases when tumor resection is incomplete, subsequent radiotherapy may be utilized to prevent recurrence or metastasis.[45]

Radiofrequency ablation of the tumor is an alternative to radical surgical resection and may be considered in selected patients for functional salvage, especially in tumors occurring in the extremities.[46] Prompt symptom control usually follows radiofrequency ablation; however, long-term effectiveness remains unknown.

For tumors that are very difficult to detect and preclude the opportunity of surgical cure, medical therapy with phosphate supplementation and calcitriol has been used to amend phosphate depletion and vitamin D deficiency–related osteomalacia.[41] Octreotide therapy had been effective in controlling symptoms in some patients with strong expression of SSTR of the tumor.[47]

Conclusion

Despite increasing knowledge on the pathophysiology of TIO, detection of the candidate lesion causing TIO remains a clinical challenge. We recommend whole-body, head-to-toe Ga68-DOTATATE PET/CT imaging as the first-line diagnostic imaging tool in patients with clinically and laboratory-suspected TIO to avoid a delay in diagnosis. Combined focused diagnostic CT and/or MRI are imperative for accurate delineation of tumor and surgical guidance. Complete surgical resection of the tumor is curative in this disorder.

References

1. Drezner MK. Tumor-induced osteomalacia. Rev Endocr Metab Disord 2001;2:175–86.
2. Folpe AL, Fanburg-Smith JC, Billings SD, et al. Most osteomalacia-associated mesenchymal tumors are a single histopathologic entity: an analysis of 32 cases and a comprehensive review of the literature. Am J Surg Pathol 2004;28:1–30.
3. Cai Q, Hodgson SF, Kao PC, et al. Brief report: inhibition of renal phosphate transport by a tumor product in a patient with oncogenic osteomalacia. N Engl J Med 1994;330:1645–9.
4. Shimada T, Mizutani S, Muto T, et al. Cloning and characterization of FGF23 as a causative factor of tumor-induced osteomalacia. Proc Natl Acad Sci U S A 2001;98:6500–5.
5. Deep NL, Cain RB, McCullough AE, et al. Sinonasal phosphaturic mesenchymal tumor: case report and systematic review. Allergy Rhinol (Providence) 2014;5:162–7.
6. Khosravi A, Cutler CM, Kelly MH, et al. Determination of the elimination half-life of fibroblast growth factor-23. J Clin Endocrinol Metab 2007;92:2374–7.
7. Ho CL. Ga68-DOTA peptide PET/CT to detect occult mesenchymal tumor-inducing osteomalacia: a case series of three patients. Nucl Med Mol Imaging 2015;49:231–6.
8. Clifton-Bligh RJ, Hofman MS, Duncan E, et al. Improving diagnosis of tumor-induced osteomalacia with Gallium-68 DOTATATE PET/CT. J Clin Endocrinol Metab 2013;98:687–94.
9. Mc CR. Osteomalacia with Looser's nodes (Milkman's syndrome) due to a raised resistance to vitamin D acquired about the age of 15 years. Q J Med 1947;16:33–46.
10. Chong WH, Yavuz S, Patel SM, et al. The importance of whole body imaging in tumor-induced osteomalacia. J Clin Endocrinol Metab 2011;96:3599–600.
11. Jiang Y, Xia WB, Xing XP, et al. Tumor-induced osteomalacia: an important cause of adult-onset hypophosphatemic osteomalacia in China: report of 39 cases and review of the literature. J Bone Miner Res 2012;27:1967–75.
12. Dadoniene J, Miglinas M, Miltiniene D, et al. Tumour-induced osteomalacia: a literature review and a case report. World J Surg Oncol 2016;14:4.
13. Hu FK, Yuan F, Jiang CY, et al. Tumor-induced osteomalacia with elevated fibroblast growth factor 23: a case of phosphaturic mesenchymal tumor mixed with connective tissue variants and review of the literature. Chin J Cancer 2011;30:794–804.
14. Renkema KY, Alexander RT, Bindels RJ, et al. Calcium and phosphate homeostasis: concerted interplay of new regulators. Ann Med 2008;40:82–91.
15. Sommer S, Berndt T, Craig T, et al. The phosphatonins and the regulation of phosphate transport and vitamin D metabolism. J Steroid Biochem Mol Biol 2007;103:497–503.
16. Meyer RA Jr., Meyer MH, Gray RW. Parabiosis suggests a humoral factor is involved in X-linked hypophosphatemia in mice. J Bone Miner Res 1989;4:493–500.
17. Liu S, Quarles LD. How fibroblast growth factor 23 works. J Am Soc Nephrol 2007;18:1637–47.
18. Hannan FM, Athanasou NA, Teh J, et al. Oncogenic hypophosphataemic osteomalacia: biomarker roles of fibroblast growth factor 23, 1,25-dihydroxyvitamin D3 and lymphatic vessel endothelial hyaluronan receptor 1. Eur J Endocrinol 2008;158:265–71.
19. Shimada T, Hasegawa H, Yamazaki Y, et al. FGF-23 is a potent regulator of vitamin D metabolism and phosphate homeostasis. J Bone Miner Res 2004;19:429–35.
20. Weidner N. Review and update: oncogenic osteomalacia-rickets. Ultrastruct Pathol 1991;15:317–33.
21. Carpenter TO. Oncogenic osteomalacia——a complex dance of factors. N Engl J Med 2003;348:1705–8.
22. Jan de Beur SM. Tumor-induced osteomalacia. JAMA 2005;294:1260–7.
23. Duet M, Kerkeni S, Sfar R, et al. Clinical impact of somatostatin receptor scintigraphy in the management of tumor-induced osteomalacia. Clin Nucl Med 2008;33:752–6.
24. Haeusler G, Freilinger M, Dominkus M, et al. Tumor-induced hypophosphatemic rickets in an adolescent boy–clinical presentation, diagnosis, and histological findings in growth plate and muscle tissue. J Clin Endocrinol Metab 2010;95:4511–7.
25. Meyer RA Jr., Conway WF, Chan JC. X-linked hypophosphatemia. Semin Nephrol 1989;9:56–61.
26. Quarles LD. FGF23, PHEX, and MEPE regulation of phosphate homeostasis and skeletal mineralization. Am J Physiol Endocrinol Metab 2003;285:E1–9.
27. Quarles LD, Drezner MK. Pathophysiology of X-linked hypophosphatemia, tumor-induced osteomalacia, and autosomal dominant hypophosphatemia: a perPHEXing problem. J Clin Endocrinol Metab 2001;86:494–6.
28. Fukumoto S, Takeuchi Y, Nagano A, et al. Diagnostic utility of magnetic resonance imaging skeletal survey in a patient with oncogenic osteomalacia. Bone 1999;25:375–7.
29. Sood A, Agarwal K, Shukla J, et al. Bone scintigraphic patterns in patients of tumor induced osteomalacia. Indian J Nucl Med 2013;28:173–5.
30. Lee HK, Sung WW, Solodnik P, et al. Bone scan in tumor-induced osteomalacia. J Nucl Med 1995;36:247–9.
31. Hodgson SF, Clarke BL, Tebben PJ, et al. Oncogenic osteomalacia: localization of underlying peripheral mesenchymal tumors with use of Tc 99m sestamibi scintigraphy. Endocr Pract 2006;12:35–42.
32. Kimizuka T, Ozaki Y, Sumi Y. Usefulness of 201Tl and 99mTc MIBI scintigraphy in a case of oncogenic osteomalacia. Ann Nucl Med 2004;18:63–7.
33. Dupond JL, Mahammedi H, Prie D, et al. Oncogenic osteomalacia: diagnostic importance of fibroblast growth factor 23 and F-18 fluorodeoxyglucose PET/CT scan for the diagnosis and follow-up in one case. Bone 2005;36:375–8.
34. Jagtap VS, Sarathi V, Lila AR, et al. Tumor-induced osteomalacia: a single center experience. Endocr Pract 2011;17:177–84.
35. Seo HJ, Choi YJ, Kim HJ, et al. Using (18)F-FDG PET/CT to detect an occult mesenchymal tumor causing oncogenic osteomalacia. Nucl Med Mol Imaging 2011;45:233–7.
36. Garcia CA, Spencer RP. Bone and In-111 octreotide imaging in oncogenic osteomalacia: a case report. Clin Nucl Med 2002;27:582–3.
37. Jan de Beur SM, Streeten EA, Civelek AC, et al. Localisation of mesenchymal tumours by somatostatin receptor imaging. Lancet 2002;359:761–3.

38. Hendry DS, Wissman R. Case 165: oncogenic osteomalacia. Radiology 2011;258:320–2.
39. Hesse E, Moessinger E, Rosenthal H, et al. Oncogenic osteomalacia: exact tumor localization by co-registration of positron emission and computed tomography. J Bone Miner Res 2007;22:158–62.
40. von Falck C, Rodt T, Rosenthal H, et al. (68)Ga-DOTANOC PET/CT for the detection of a mesenchymal tumor causing oncogenic osteomalacia. Eur J Nucl Med Mol Imaging 2008;35:1034.
41. Chong WH, Molinolo AA, Chen CC, et al. Tumor-induced osteomalacia. Endocr Relat Cancer 2011;18:R53–77.
42. Agrawal K, Bhadada S, Mittal BR, et al. Comparison of 18F-FDG and 68Ga DOTATATE PET/CT in localization of tumor causing oncogenic osteomalacia. Clin Nucl Med 2015;40:e6–e10.
43. Clunie GP, Fox PE, Stamp TC. Four cases of acquired hypophosphataemic ('oncogenic') osteomalacia. Problems of diagnosis, treatment and long-term management. Rheumatology 2000;39:1415–21.
44. Ogose A, Hotta T, Emura I, et al. Recurrent malignant variant of phosphaturic mesenchymal tumor with oncogenic osteomalacia. Skeletal Radiol 2001;30:99–103.
45. Hautmann AH, Schroeder J, Wild P, et al. Tumor-induced osteomalacia: increased level of FGF-23 in a patient with a phosphaturic mesenchymal tumor at the tibia expressing periostin. Case Rep Endocrinol 2014 https://doi.org/10.1155/2014/729387.
46. Hesse E, Rosenthal H, Bastian L. Radiofrequency ablation of a tumor causing oncogenic osteomalacia. N Engl J Med 2007;357:422–4.
47. Seufert J, Ebert K, Muller J, et al. Octreotide therapy for tumor-induced osteomalacia. N Engl J Med 2001;345:1883–8.